Molecular Conformations and Magnetic Parameters of the Compact Trimethylenemethane–Type Triplet Diradical

ARTICLE *in* THE JOURNAL OF PHYSICAL CHEMISTRY A · JULY 2013

Impact Factor: 2.69 · DOI: 10.1021/jp405572n · Source: PubMed

7 AUTHORS, INCLUDING:

Eugenii Ya Misochko
Russian Academy of Sciences
65 PUBLICATIONS **526** CITATIONS
SEE PROFILE

Denis V. Korchagin
Russian Academy of Sciences
45 PUBLICATIONS **146** CITATIONS
SEE PROFILE

Svyatoslav Tolstikov
Novosibirsk State University
27 PUBLICATIONS **86** CITATIONS
SEE PROFILE

Evgeny Tretyakov
Novosibirsk Institute of Organic Chemistry
126 PUBLICATIONS **858** CITATIONS
SEE PROFILE

THE JOURNAL OF PHYSICAL CHEMISTRY A

Article

pubs.acs.org/JPCA

Molecular Conformations and Magnetic Parameters of the Compact Trimethylenemethane-Type Triplet Diradical

Eugenii Ya. Misochko,*[,†] Denis V. Korchagin,[†] Alexander V. Akimov,[†] Artem A. Masitov,[†] Svyatoslav E. Tolstikov,[‡] Evgeny V. Tretyakov,[‡] and Victor I. Ovcharenko[‡]

[†]Institute of Problems of Chemical Physics, Russian Academy of Sciences, 142432 Chernogolovka, Moscow Region, Russian Federation

[‡]International Tomography Center, Siberian Branch of the Russian Academy of Sciences, Institutskaya Street 3a, 630090 Novosibirsk, Russian Federation

Supporting Information

ABSTRACT: The ESR spectrum of compact nitroxide (NO)-substituted nitronyl nitroxide (NN) triplet diradical *N-tert*-butyl-*N*-oxidanyl-2-amino-4,4,5,5-tetramethyl-4,5-dihydro-1*H*-imidazole-3-oxide-1-oxyl (**1**) was recorded in solid argon matrix at 15 K. The zero-field splitting (ZFS) parameters of **1** were derived from the recorded ESR spectrum: $|D| = 0.0248$ cm^{-1} and $E = 0.0025$ cm^{-1}. Quantum chemical calculations have been performed using DFT and multiconfigurational ab initio (CAS) methods in order to establish equilibrium geometries of the conformational isomers resulting from twisted conformations of NO and NN moieties. The ZFS parameters of **1** were calculated at these levels of theory to test validity of the calculated structures. The calculation results were analyzed using the measured ZFS parameters and magnetic and structural data from the previous studies (Suzuki, S.; et al. *J. Am. Chem. Soc.* **2010**, *132*, 15908; Tretyakov, E. V.; et al. *Russ. Chem. Bull.* **2011**, *60*, 2608). It was found that the ab initio method is most successful for accurate predictions of molecular and magnetic parameters. Diradical **1** has only one stable enantiomeric pair in pseudoeclipsed conformations. The two chiral isomers exist in racemic crystals **1** and in solid matrices with molecular parameters close to those attributed to a free molecule. The analysis of the spin density distribution suggests that one unpaired electron occupies NO group at the equilibrium geometry, whereas the torsion of NO group governs the spin density distribution of the second unpaired electron on a conjugated fragment in NN group. The increase in planarity by torsion of NO group enhances the trimethylenemethane-type properties and, therefore, gives rise to larger ferromagnetic exchange interaction. More planar equilibrium geometry and greater (three times) exchange interaction constant J were predicted for hypothetical diradical **1a**, where bulky *tert*-butyl group is replaced by a methyl group in the nitroxide fragment.

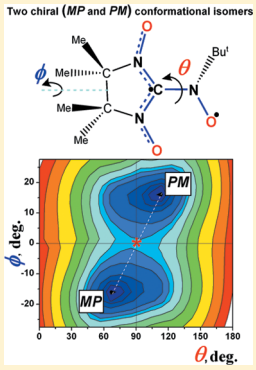

1. INTRODUCTION

Diradicals with strong intramolecular ferromagnetic coupling constitute one of the prerequisites for design of organic molecular magnets. A variety of organic stable neutral radicals have been used as spin sources to generate ferromagnetic exchange interactions in diradical systems.[1,2] Also, diverse couplers that link two radicals were investigated theoretically and experimentally. Most of these studies focused on the search for diradical molecules with large intramolecular ferromagnetic interactions that are synthetically affordable.[3−10] Recently, highly compact triplet nitroxide (NO)-substituted nitronyl nitroxide (NN) diradical *N-tert*-butyl-*N*-oxidanyl-2-amino-4,4,5,5-tetramethyl-4,5-dihydro-1*H*-imidazole-3-oxide-1-oxyl (**1**) was reported.[11,12] It was experimentally shown that diradical **1** is stable under air conditions at room temperature and has large ferromagnetic exchange interaction constant $J/k_B \approx +400$ K ($\boldsymbol{H} = -2J\mathbf{S}_{1/2} \bullet \mathbf{S}_{1/2}$). Notably, diradical **1** has the isoelectronic structure with trimethylenemethane (TMM) that explains a high positive value of J.

The molecular structure of diradical **1** includes two flexible moieties causing four conformational isomers. The first conformationally significant feature of **1** is the torsion of nitroxide group around the C2−N1 bond. The torsion angle θ is described by dihedral angle between the (N2−C2−N3) and (C2−N1−O1) planes. The second conformationally sensitive moiety of **1** has a twisted (out-of-plane) distortion of the imidazolyl ring being common to all α-nitronyl nitroxides. Usually, the conformation of the imidazolyl ring in α-NN radicals is described by the twisted angle ϕ between the C3−C4 bond and the plane formed by the N2−C2−N3 unit in the ring.[13,14] The chiral information inherent in the conformational parameters ϕ and θ (given by the sign of both parameters) suggests four possible gross conformations, shown in Figure 1. The conformational isomers contain two enantiomeric pairs: (MP, PM) and (PP, MM), where P stands for "plus" and M stands for "minus". As a rule, intermolecular interactions govern the conformational structures and molecular parameters in

Received: June 5, 2013
Revised: July 26, 2013
Published: July 29, 2013

dx.doi.org/10.1021/jp405572n | *J. Phys. Chem. A* 2013, 117, 8065−8072

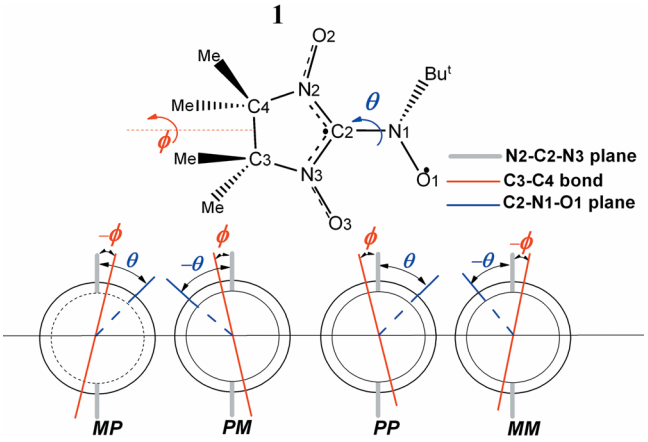

Figure 1. General formula of diradical **1** along with a schematic view of four possible diastereomers in pseudoeclipsed (MP, PM) and pseudo-*anti* (PP, MM) conformations.

molecular crystals of NN-based radicals due to high flexibility of these moieties.[1,14]

In contrast to the previously studied NN-based molecules, diradical **1** has a compact molecular structure. The compact NO radical is directly connected to the NN radical without any coupler. Thus, one can expect that molecular structures in crystal **1** can be close to that in a free molecule. In this study, we attempted to rationalize the effects of conformational stereochemistry in diradical **1**, since the torsion angle θ fixes spatial arrangement of spin containing groups and is of great importance for unraveling magnetic properties of the TMM-type diradicals.[3,4,6] In order to obtain high spectral resolution in ESR measurements and to minimize the impact of the environment, we used a matrix isolation ESR technique.[15] We recorded ESR spectra of **1** in solid argon matrices at 15 K and determined its zero-field splitting (ZFS) parameters D and E. These parameters both are structurally sensitive features of diradical systems. Further, we used the ZFS parameters to probe molecular structures obtained with quantum chemical DFT and ab initio calculations. Also, the calculation results were analyzed using magnetic and structural data from the previous studies.[11,12] The results of the present study showed that diradical **1** has only one stable enantiomeric pair in pseudoeclipsed (PM, MP) conformations. The two chiral isomers exist in racemic crystals **1** and in solid matrices with molecular parameters close to those attributed to a free molecule.

2. METHODS

2.1. Experimental Section. Diradical **1** was synthesized according to the literature procedure.[12] The experimental technique and apparatus for low-temperature matrix-isolation ESR spectroscopy have been described previously.[16] Solid argon films doped with powder **1** were prepared by vacuum codeposition of two separate molecular beams (Ar and **1** vapor) onto a substrate (sapphire rod) held at 15 K in a high-vacuum chamber. The gas beams were deposited from two spatially separated ports onto the lower part of a flat sapphire rod (2 × 4 × 50 mm, deposition area was 4 × 5 mm^2). The **1** vapor was produced by an oven heated to ∼60 °C. The oven temperature was regulated by a precise temperature controller and was chosen to obtain the ratio **1**/Ar < 10^{-3}. The rate of deposition was estimated in separate experiments by determining the sample thickness using an interferometric method. The interference fringes due to the sample−vacuum and the sample−sapphire interfaces were recorded for a pure **1** sample during the deposition of its vapor using a He−Ne laser beam. Based on the number of the measured interference fringes, the rate of **1** deposition was estimated. The gas flow rate from the argon channel was adjusted by a needle valve and measured by a manometer. The deposition rate was typically 10 μmol/min, and the thickness of the deposited argon films was typically 100 μm. Temperature stability of the samples was ∼0.1 K over a 12−40 K range. ESR spectra were recorded using a standard 9 GHz spectrometer at enough low microwave power to avoid the saturation effects.

2.2. Computational Methods. The equilibrium geometries of diastereomeric conformers **1** were optimized using the unrestricted DFT approach at B3LYP/6-311G(d,p) level of theory and multiconfigurational ab initio (complete active space, CAS) method with the TZVP basis set by the Gaussian 03 program.[17] The active space in CAS calculations was composed as (4,4) that accounts for a complete set of four valence π-orbitals (see Supporting Information). Given that the twisted angles θ and ϕ are important degrees of freedom for diradical **1**, we studied properties of the system as a function of these angles. Full and constrained (at fixed parameters θ and ϕ) optimizations were performed at these levels of theory.

Different quantum chemical methods were applied for calculations of the ZFS parameters. The ZFS parameters were calculated by the ORCA program package[18] with two approaches based on McWeeny−Mizuno[19,20] and multi-configurational ab initio formalisms.[21,22] One-electron spin density matrices for evaluation of the spin−spin part of the D-tensor in the McWeeny−Mizuno equation have been obtained from unrestricted DFT spin matrices. In the second case, the D-tensor (including both spin−spin and spin−orbit contributions) was obtained employing the ab initio CAS approach. The spin−spin contribution was evaluated using a two-electron spin−spin coupling operator over many-electron wave functions as described earlier.[21,22] DFT calculations of the ZFS parameters carried out with the functional PBE and DZ basis showed good results in the previous test calculations for various organic high-spin molecules.[23] All ab initio calculations of ZFS parameters were performed with electronic basis set SVP. Preliminary calculations revealed no sufficient influence of the size of the basis set and the reference wave functions on the accuracy of the calculated parameters.[23] The natural resonance theory analysis was performed using NBO 6.0 program.[24] Multiconfigurational CAS calculations of Mayer bond orders[25] were performed by Orca program package.

3. RESULTS AND DISCUSSION

3.1. Powder ESR Spectra and ZFS Parameters. The EPR spectrum of freshly prepared **1**/Ar sample is shown in Figure 2a. The spectrum exhibits six broad ESR lines (z_1, x_1, y_1, x_2, y_2, and z_2), attributable to randomly oriented triplet species. All of these six lines are characterized by strong inhomogeneous broadening. A half-field signal assigned to $|\Delta m_s| = 2$ transition in triplet molecules was recorded at magnetic field 161.5 mT. Additionally, the spectrum shows a series of narrow EPR lines in the region of free electron g-factor g_e (shown in the inset). The shape and structure of this series of lines represent a typical anisotropic spectrum of frozen α-NN-radicals with hyperfine splitting on two nitrogen atoms; see, for example, ref 26. Figure 2b shows changes in ESR spectra as a result of annealing a

dx.doi.org/10.1021/jp405572n | J. Phys. Chem. A 2013, 117, 8065−8072

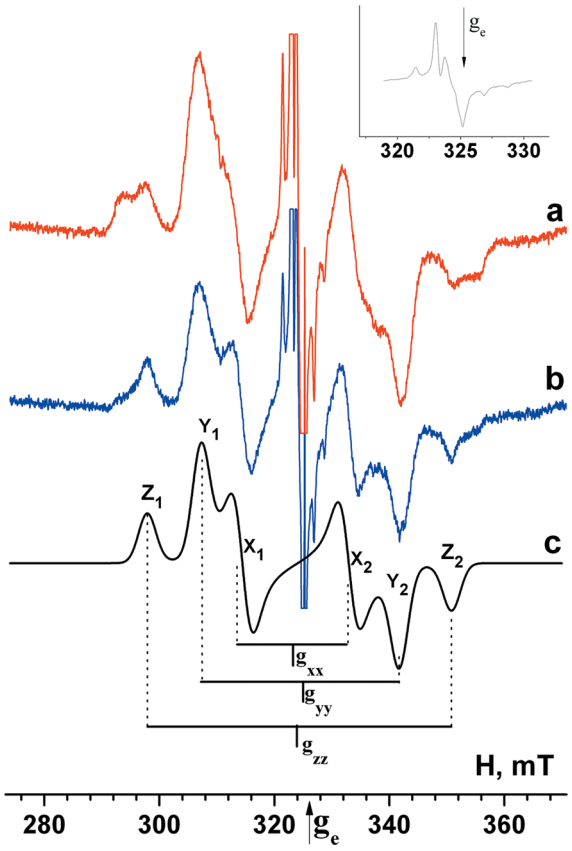

Figure 2. ESR spectra of the deposited sample Ar/**1** ≈ 10^4 after preparation at 15 K (a) and after subsequent annealing at 28 K (b). The spectra were recorded at 15 K. Microwave frequency ν_0 = 9.107 290 GHz. The simulated powder spectrum of the triplet diradical with ZFS parameters D = 0.0248 cm^{-1}, E = 0.0025 cm^{-1}, and g = [2.0080; 2.0039; 2.0060] (c). The center of the spectrum (b) is shown in the inset.

sample at 28 K. The spectrum 2b demonstrates that the ESR lines of triplet species become narrower and well resolved after annealing. Thus, freshly deposited samples contain several nonequilibrium structural configurations of diradical **1** (i.e., typical matrix site-splitting for floppy molecular structures). These frozen configurations relax upon annealing of a sample. The stable configuration of **1** demonstrates the spectrally resolved splitting of the perpendicular components X_i and Y_i. This fact suggests that ZFS has nonvanishing ZFS parameter E. The intensities of EPR lines obeyed the Curie law, hence confirming the ground triplet state for diradical **1**.

The ZFS parameters for diradical **1** were determined by the comparison of the simulated and experimentally obtained ESR spectra. This procedure was described in detail in ref 16. Simulations were performed using the *EasySpin* program package,[27] operating with an exact numerical matrix diagonalization analysis of the spin Hamiltonian (1) for randomly oriented species with S = 1.

$$H = g\beta HS + DS_z^2 + E(S_x^2 - S_y^2) \quad (1)$$

As starting parameters, we first considered the anisotropic parameters of the **g**-tensor, g_{xx}, g_{yy}, and g_{zz}, as the middle points between the corresponding components in the spectrum, see Figure 1c. The ZFS parameters D and E yielding the best approximation were evaluated by minimization of the functional R, which was defined as the root-mean-square (rms) deviation of calculated resonance fields from those measured experimentally. The final shape of the simulated spectrum was obtained with the optimization procedure in the *EasySpin* package implemented. The spectrum optimized was obtained at D = |0.0248| cm^{-1} and E = |0.0025| cm^{-1} corresponding to the rms deviation of R(min) = 0.7 mT (Figure 2c) with the line width of 3 mT. This D value of **1** is very close to the previously measured D values of **1** in frozen organic glasses.[11,12] The obtained parameter E = 0.0025 cm^{-1} in solid argon matrices is ca. 40% higher than those measured previously, presumably due to much better spectral resolution of the perpendicular components in an argon matrix.

3.2. Structural Calculations. As the first step, we calculated potential energy surface (PES) for triplet **1** by using the DFT method. We calculated the optimized geometries at full optimization procedure as well as at fixed angles θ and ϕ. The obtained plot of PES is shown in Figure 3A. It implies four equilibrium configurations corresponding to

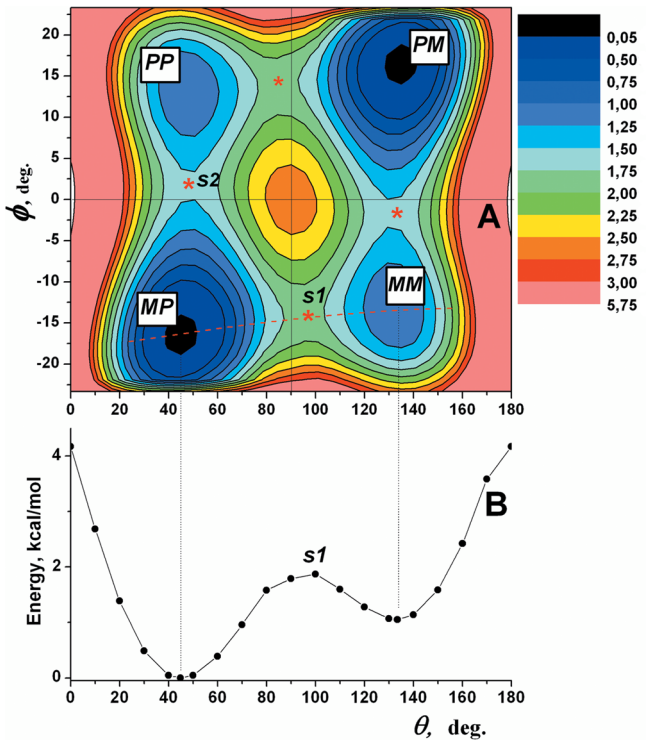

Figure 3. (A) DFT-calculated PES for diradical **1** in the ground triplet state. The energies are given in kcal/mol. Saddle points S1 and S2 are marked with (*). (B). Calculated energies along the minimum energy pathway (MEP) shown with dashed red line.

the pseudoeclipsed (PM, MP) with θ^* = 44.9° and ϕ^* = −16.6° and pseudo-*anti* (PP, MM) conformations with θ^* = 133.4° and ϕ^* = −13.7°. The pseudoeclipsed (PM, MP) conformation is 1.0 kcal/mol (0.8 kcal/mol including the zero-point energy (ZPE)) more stable, see Figure 3B. Two saddle points S1 and S2 suggest energy barriers for intramolecular transformations MP → MM being ca. 1.9 kcal/mol (1.6 kcal/mol including ZPE) and MP → PP being ca. 1.6 kcal/mol (1.5 kcal/mol including ZPE), respectively. A series of DFT calculations with extended electronic basis sets 6-311+G-(2d,2p) and 6-311++G(3df,3pd) revealed almost the same local minima. The barriers for intramolecular transformations MP → MM and MP → PP are lower: 1.2 and 1.4 kcal/mol,

dx.doi.org/10.1021/jp405572n | J. Phys. Chem. A 2013, 117, 8065−8072

respectively (the details are given in the Supporting Information). Thus, these calculations testified on extremely low barriers for transformations to the global minimum (less than 0.5 kcal/mol). The calculated equilibrium geometries are far from those obtained previously with X-ray diffraction measurements for crystals **1**. According to the crystallographic data, the molecular and packing structures of **1** correspond to the enantiomers MP and PM with angles θ_1 = 65.4° and ϕ_1 = 13.9° (CIF data[11]). According to the data in ref 12, the torsion angle θ_1 equals 69.4°.

To check the validity of DFT calculations, we calculated PES with a more sophisticated CAS method. The obtained fully optimized structures showed that only one pair of chiral conformers MP and PM are stable at this level of theory. The equilibrium geometry corresponds to the torsion angle θ_1 = 66° and twisted angle ϕ_1 = −16.5°. These parameters are both very close to those determined with X-ray diffraction measurements for crystals **1**. Calculations of the total PES with constrained CAS optimizations (at fixed θ and ϕ) appear to be computationally rather expensive. Fortunately, several test calculations revealed that the constrained optimizations with DFT and CAS methods give practically similar molecular parameters. Therefore, we used the DFT geometries to calculate the PES shown in Figure 4A. To confirm the validity of the calculated PES, we performed a set of constrained optimizations with the CASSCF method shown in Figure 4B. The calculations suggest a saddle point at a high symmetrical orthogonal configuration (θ = 90° and ϕ = 0°). The saddle point corresponds to the energy barrier of 1.2 kcal/mol for interconversion: MP ↔ PM. Compared to the DFT calculations, the ab initio method predicts stronger repulsive forces where the twisted angle θ moves to planar configurations, θ < 50° and θ > 120°. On the other hand, DFT calculations overestimate the interaction energy in the vicinity of the orthogonal configuration at θ = 90°. Likely, the neglect of two-electron correlations in DFT calculations (that is significant for TMM systems) results in the spurious stationary points shown in Figure 3. It is known that most standard quantum chemical one-configurational methods may appear difficult when describing diradicals, where more than one-electron configuration significantly contributes to a wave function.[28−30]

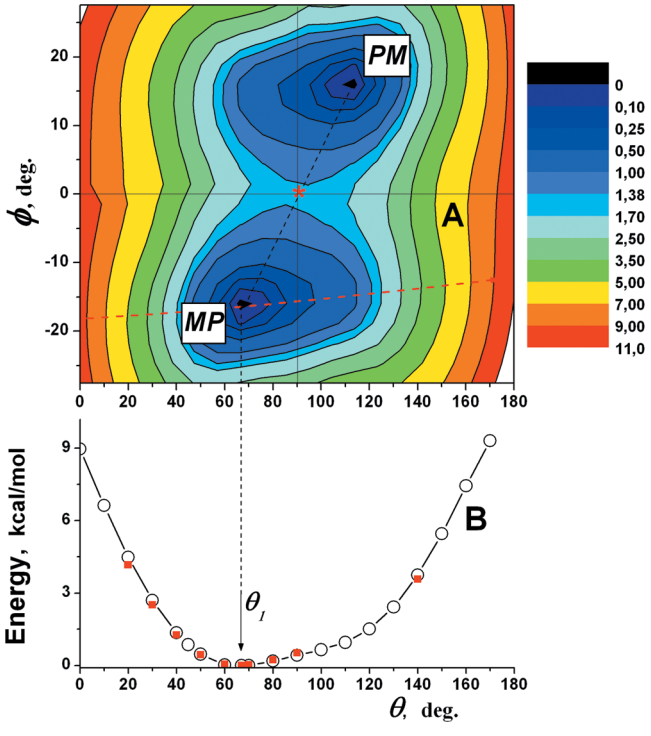

Figure 4. (A) Calculated PES (CAS) for diradical **1** in the ground triplet state. The equilibrium configurations were obtained at full CAS optimization procedure. Total PES was obtained using molecular geometries from the constrained DFT optimizations. The saddle point is marked with (*). (B) Calculated energies are given as a function of angle θ along the pathway shown with dashed red line. Energies from constrained geometry optimizations with the CASSCF method are shown with red squares.

3.3. Calculations of the ZFS Parameters. The results of quantum chemical calculations for ZFS parameters as a function of angle θ are graphically shown in Figure 5. Both

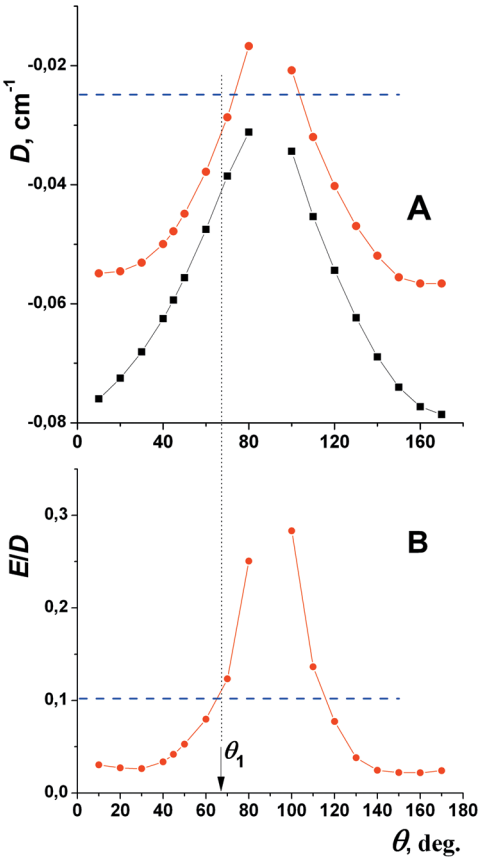

Figure 5. Calculated ZFS parameters D (A) and E/D (B) at different torsion angles θ. DFT calculation data are shown with dark squares. Ab initio (CAS) calculations are shown with red circles. The experimental values of D and E/D are shown with horizontal dashed lines. Torsion angle θ_1 = 66° corresponds to the equilibrium configuration in Figure 4.

DFT and ab initio calculations predict a negative sign for D in accordance with previous calculations.[11,12] Note that the prediction of the sign and magnitude of D is not straightforward in the vicinity of the orthogonal configuration at 80° < θ < 110° because parameter D becomes ambiguous where E/D approaches the rhombic limit E/D = 1/3; see the Supporting Information. Figure 5A demonstrates that the DFT method overestimates the magnitudes of D for all config-

dx.doi.org/10.1021/jp405572n | J. Phys. Chem. A 2013, 117, 8065−8072

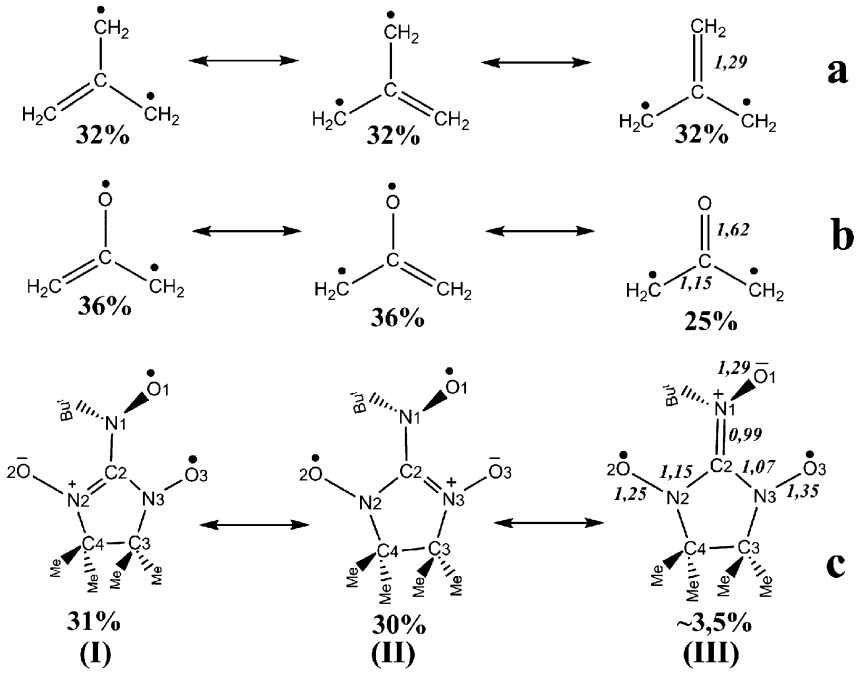

Figure 6. Dominant resonance structures for the α-spins of triplet TMM-type diradicals: (a) TMM with molecular parameters taken from ref 31; (b) oxyallyl with molecular parameters taken from ref 32; (c) diradical **1** with equilibrium CAS configuration. Diradical-like structures **I**–**III** constitute ca. 64% of the overall wave function in diradical **1**. A number of other Lewis structures are revealed, but each contributes less than 1.5% to the overall structure. The calculated Mayer bond orders for the conjugated bonds are shown with italic symbols in the structures **III**.

urations. Beside this, the DFT calculated parameters E/D = 0.20–0.30 considerably exceed the experimental value. Ab initio (CAS) calculations improve the predictions of D and E/D relative to the experimental values. Calculations predict the parameters $D = -0.029$ cm^{-1} and $E/D = 0.11$ at the equilibrium configuration ($\theta_1 = 66°$ and $\phi_1 = -16.5°$). These parameters both lie very close to those determined by ESR measurement in argon matrices. These results allowed us to conclude that diradical **1** has only one stable enantiomeric pair in PM and MP conformations. The two chiral isomers exist in solid matrices, as well as in racemic crystals **1** with molecular parameters close to those attributed to a free molecule. Note that the enantiomeric pair PM and MP is most statistically probable for the family of phenyl α-nitronyl nitroxides.[14]

3.4. Spin Density Distribution and TMM-Type Properties of Diradical 1. At simple consideration, TMM-type diradicals comprise three main resonance structures, which form a cross-conjugated π-system. The latter provides a strong delocalization of both unpaired electrons and thus determines magnetic parameters (such as J, D, and E/D). Figure 6 gives the important resonance structures for several diradicals of TMM-family obtained with natural resonance theory (NRT) and DFT spin density matrices.[33] The NRT analysis suggested extremely low contribution of structure **III** to diradical **1**. Consequently, one can expect strong localization of an unpaired electron over NO group (N1O1) in **1**. To analyze the delocalization of unpaired electrons, we calculated the spin populations on atoms in **1** with CAS approach. Figure 7 shows the dependences of the spin populations on key atoms against the magnitude of torsion angle θ. In fact, the calculations showed that the spin population on NO group ρ(N1O1) = 0.97 is close to 1 at the equilibrium geometry. The maximal spin density is located on oxygen atom O1, ρ(O1) ≈ 0.75. Contrarily, the spin density distributions on the conjugated fragment O2–N2–C2–N3–O3 in NN group strongly depend

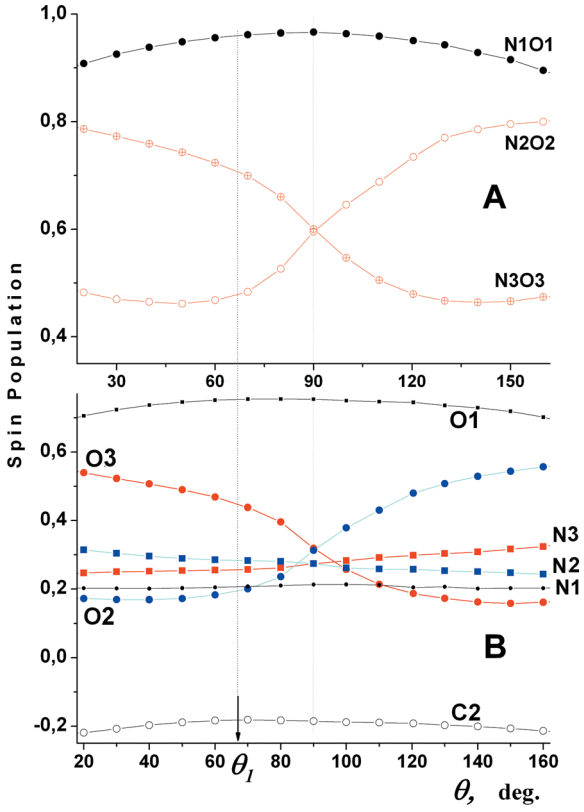

Figure 7. Mulliken spin populations (CAS) on NO groups (A) and spin-containing atoms (B) in diradical **1**. Torsion angle $\theta_1 = 66°$ corresponds to the equilibrium configuration in Figure 4.

on torsion angle θ. The decrease of spin population on N2O2 group correlates with the increase of spin population on the opposite N3O3 group where the angle θ moves to a planar

dx.doi.org/10.1021/jp405572n | J. Phys. Chem. A 2013, 117, 8065–8072

configuration (θ < 90°). Consequently, the calculations predicted substantial differences in spin populations on two NO groups (N2O2 and N3O3) in NN fragment. These calculations clearly show that the orientation of NO group governs the spin density distribution of the second unpaired electron on the conjugated fragment O2−N2−C2−N3−O3 in NN group. Notably, the deviations of angle θ from 90° to the right or to the left in Figure 7 give almost symmetric redistribution of spin densities between N2O2 and N3O3 groups. Therefore, dependences $\rho_i(\theta)$ and $D(\theta)$ are conformationally symmetric, despite the asymmetric PES at θ < 90° and θ > 90°. High negative spin density is predicted for carbon atom C2, ρ(C2) ≈ −0.22. The corresponding excess of the positive spin density appears on the N2O2 and N3O3 groups (ρ(N2O2) + ρ(N3O3) ≈ 1.25) resulting from strong spin polarization effects in the conjugated fragment O2−N2−C2−N3−O3. On the other hand, the localization of one unpaired electron on NO group (N1O1) suggests weak conjugation of C2−N1 bond, where the single bond character is dominant. The calculated extremely low (<1.00) Mayer bond order for C2−N1 bond in **1**, see Figure 6, is in line with this conclusion. Additionally, this correlates with high torsional flexibility of C2−N1 bond, which results in a very low conformational barrier and large equilibrium angle θ_1 = 66°.

We used the broken symmetry unrestricted density functional theoretical (BS-UDFT) approach proposed by Noodleman[34,35] to estimate magnetic exchange coupling constant J in diradical systems. Calculations were performed using the useful form proposed by Yamaguchi and co-workers[36]

$$J = \frac{E_{BS} - E_T}{\langle S^2\rangle_T - \langle S^2\rangle_{BS}}$$

where E_{BS}/E_T and $\langle S^2\rangle_{BS}/\langle S^2\rangle_T$ are the energy and average spin square values of the BS/triplet state, respectively. Figure 8 demonstrates the calculated J values at different torsion angles θ.

The calculated value J/k_B = 570 K at the equilibrium CAS geometry (θ_1 = 66°) is in reasonable agreement with the J value in crystals **1** measured previously.[11,12] This plot shows that the increase of planarity of the molecule stimulates strong ferromagnetic interaction. Simultaneously, the increase of planarity enhances the cross-conjugating properties of TMM-type diradical that is manifested in slight increase of the Mayer bond order of C2−N1 bond, as well as in the decrease of spin population on NO group. Such magneto−structural correlations agree with previous results for a series of TMM-family, where various types of radicals were attached to 1,1-ethenyl or cyclic structures, such as dihydropentafulvenes and cyclobutenes.[3−6] Apparently, the bulky *tert*-butyl group in NO fragment of **1** causes steric limitations for molecular planarity of **1**. To verify this effect, we performed the geometry optimization with the CAS approach for diradical **1a**, where the bulky *tert*-butyl group is replaced by a methyl group in the nitroxide fragment. This replacement lead to a smaller equilibrium angle θ_2 = 42.3°; see Figure 8. The calculations suggested much greater (three times!) intramolecular ferromagnetic exchange interaction constant J in diradical **1a** than that in **1** that is attributed to a smaller dihedral angle θ at the equilibrium configuration.

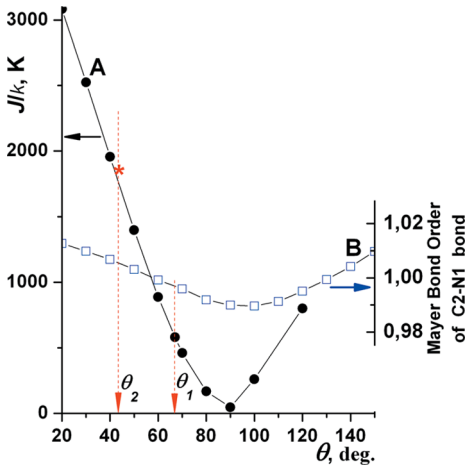

Figure 8. Calculated exchange coupling constant J (A) and Mayer bond order of C2−N1 bond (B) in diradical **1**. Torsion angle θ_1 = 66° corresponds to the equilibrium configuration in Figure 4. Torsion angle θ_2 = 42.3° corresponds to the equilibrium CAS configuration in diradical **1a**, where *tert*-butyl group in **NO** radical is replaced by a methyl group. The calculated J value in the equilibrium configuration of **1a** is shown with red asterisk (*).

4. CONCLUSIONS

The results of this study showed that the multiconfigurational ab initio method (CAS) can be successfully used for the estimation of molecular and magnetic parameters of the molecule with highly delocalized two unpaired electrons. Diradical **1** has only one stable enantiomeric pair in pseudoeclipsed (MP, PM) conformations at this level of theory. The equilibrium geometry corresponds to the torsion angle of NO group θ_1 = 66° and twisted angle in the imidazolyl ring ϕ_1 = −16.5°. Both these parameters are very close to those determined previously by means of X-ray diffraction measurements for crystals **1**. The calculated ZFS parameters D and E/D at the equilibrium geometry lie very close to those derived from ESR spectra of **1** in solid argon matrices, thus confirming identical molecular parameters of **1** in crystals and in solid matrices. Based on these data, we concluded that two chiral isomers of **1** exist in racemic crystals and solid matrices with molecular parameters close to those attributed to a free molecule.

The analysis of the electron spin density distribution showed that one unpaired electron occupies NO group (ρ(N1O1) = 0.97) at the equilibrium geometry, whereas the torsion of NO group around the C2−N1 bond governs the spin density distribution of the second unpaired electron on a conjugated fragment in the NN group. The increase of planarity enhances the TMM-type properties and thus gives rise to larger ferromagnetic exchange interaction. The more planar equilibrium geometry and the greater (by three times) exchange interaction constant J are predicted for hypothetical diradical **1a**, where bulky *tert*-butyl group is replaced by a methyl group in the nitroxide fragment.

■ ASSOCIATED CONTENT

Supporting Information

(1) Cartesian coordinates of CASSCF optimized diradicals **1** and **1a**; (2) frontier MOs of diradical **1** included in active space; (3) ZFS parameters of **1** in the vicinity of the orthogonal configuration at 80° < θ < 110°; (4) basis sets dependence in the structural DFT calculations; (5) complete ref 17. This material is available free of charge via the Internet at http://pubs.acs.org.

AUTHOR INFORMATION

Corresponding Author

*E-mail: misochko@icp.ac.ru.

Notes

The authors declare no competing financial interest.

ACKNOWLEDGMENTS

The study was supported by the Russian Foundation for Basic Research (grants 13-03-00757 and 12-03-00067), the Russian Academy of Sciences (Program OX-01), and the Council on Grants at the President of the Russian Federation (Program for State Support of Young Scientists, grant MK-5791.2013.3).

REFERENCES

(1) See recent reviews: Tretyakov, E. V.; Ovcharenko, V. I. The Chemistry of Nitroxide Radicals in the Molecular Design of Magnets. *Russ. Chem. Rev.* **2009**, *78*, 971−1009.

(2) Baumgarten, M. High Spin Molecules Directed Towards Molecular Magnets. In *EPR of Free Radicals in Solids I, Progress in Theoretical Chemistry and Physics*; Lund, A., Shiotani, M., Eds.; Springer, Science+Business Media: Dordrecht, Germany, 2013; Vol. *24*, pp 205−243.

(3) Shultz, D. A.; Fico, R. M., Jr.; Lee, H.; Kampf, J. W.; Kirschbaum, K.; Pinkerton, A. A.; Boyle, P. D. Mechanisms of Exchange Modulation in Trimethylenemethane-Type Biradicals: The Roles of Conformation and Spin Density. *J. Am. Chem. Soc.* **2003**, *125*, 15426−15432.

(4) Shultz, D. A.; Fico, R. M., Jr.; Bodnar, S. H.; Kumar, R. K.; Vostrikova, K. E.; Kampf, J. W.; Boyle, P. D. Trends in Exchange Coupling for Trimethylenemethane-Type Bis(semiquinone) Biradicals and Correlation of Magnetic Exchange with Mixed Valency for Cross-Conjugated Systems. *J. Am. Chem. Soc.* **2003**, *125*, 11761−11771.

(5) Terada, E.; Okamoto, T.; Kozaki, M.; Masaki, M. E.; Shiomi, D.; Sato, K.; Takui, T.; Okada, K. Exchange Interaction of 5,5′-(*m*- and *p*-phenylene)bis(10-phenyl-5,10-dihydrophenazine) Dications and Related Analogues. *J. Org. Chem.* **2005**, *70*, 10073−1081.

(6) Ali, Md. E.; Roy, A. S.; Datta, S. N. Molecular Tailoring and Prediction of Strongly Ferromagnetically Coupled Trimethylenemethane-Based Nitroxide Diradicals. *J. Phys. Chem. A* **2007**, *111*, 5523−5527.

(7) Latif, I. A.; Singh, V. P.; Bhattacharjee, U.; Panda, A.; Datta, S. N. Very Strongly Ferromagnetically Coupled Diradicals from Mixed Radical Centers. II. Nitronyl Nitroxide Coupled to Tetrathiafulvalene via Spacers. *J. Phys. Chem. A* **2010**, *114*, 6648−6656.

(8) Ko, K. C.; Cho, D.; Lee, J. Y. Systematic Approach to Design Organic Magnetic Molecules: Strongly Coupled Diradicals with Ethylene Coupler. *J. Phys. Chem. A* **2012**, *116*, 6837−6844.

(9) Liu, Y.; Villamena, F. A.; Rockenbauer, A.; Song, Y.; Zweier, J. L. Structural Factors Controlling the Spin−Spin Exchange Coupling: EPR Spectroscopic Studies of Highly Asymmetric Trityl−Nitroxide Biradicals. *J. Am. Chem. Soc.* **2013**, *135*, 2350−2356.

(10) Sadhukhan, T.; Hansda, S.; Pal, A. K.; Venkatakrishna, G. V.; Latif, I. A.; Datta, S. N. Theoretical Investigation of Photomagnetic Properties of Oxoverdazyl-Substituted Pyrenes. *J. Phys. Chem. A* **2013**, DOI: 10.1021/jp4022756j.

(11) Suzuki, S.; Furui, T.; Kuratsu, M.; Kozaki, M.; Shiomi, D.; Sato, K.; Takui, T.; Okada, K. J. Nitroxide-Substituted Nitronyl Nitroxide and Iminonitroxide. *J. Am. Chem. Soc.* **2010**, *132*, 15908−15910.

(12) Tretyakov, E. V.; Tolstikov, S. E.; Romanenko, G. V.; Bogomyakov, A. S.; Stass, D. V.; Maryasov, A. G.; Gritsan, N. P.; Ovcharenko, V. I. Method for the Synthesis of a Stable Heteroatom Analog of Trimethylenemethane. *Russ. Chem. Bull, Int. Ed.* **2011**, *60*, 2608−2612.

(13) Minguet, M.; Amambilino, D. B.; Wurst, K.; Veciana, J. Circular Dichroism Studies of Crystalline Chiral and Achiral α-Nitronyl Nitroxide Radicals in a KBr Matrix. *J. Chem. Soc., Perkin Trans.* **2001**, *2*, 670−676.

(14) Minguet, M.; Amambilino, D. B.; Cirujeda, J.; Wurst, K.; Mata, I.; Molins, E.; Novoa, J. J.; Veciana, J. Stereochemistry of Phenyl α-Nitronyl Nitroxide Radicals. *Chem.—Eur. J.* **2000**, *6*, 2350−2361.

(15) Baskir, E. G.; Misochko, E. Ya.; Nefedov, O. M. Spectroscopy and Structure of Free Radicals Stabilized in Cryogenic Matrices. *Russ. Chem. Rev.* **2009**, *78*, 683−715.

(16) Misochko, E. Ya.; Akimov, A. V.; Chapyshev, S. V. High Resolution Electron Paramagnetic Resonance Spectroscopy of Quintet Pyridyl-2,6-Dinitrene in Solid Argon: Magnetic Properties and Molecular Structure. *J. Chem. Phys.* **2008**, *128*, 124504 1−7.

(17) Fisch, M. J.; Trucks, G. W.; Schlegel, H. B.; Scuseria, G. E.; Robb, M. A.; Cheeseman, J. R.; Zakrzewski, V. G.; Montgomery, J. A., Jr.; Stratmann, R. E.; Burant, J. C.; et al. *Gaussian 03*, revision D.01; Gaussian, Inc.: Wallingford, CT, 2004.

(18) Neese; F. The ORCA Program System. *Wiley interdisciplinary Reviews—Computational Molecular Science*; 2012; Vol. *2*, pp 73−120. The program was downloaded from http://www.thch.uni-bonn.de/tc/orca.

(19) McWeeny, R.; Mizuno, Y. The Density Matrix in Many-Electron Quantum Mechanics. II. Separation of Space and Spin Variables; Spin Coupling Problems. *Proc. R. Soc. London, Ser. A* **1961**, *259*, 554−577.

(20) Sinnecker, S.; Neese, F. Spin−Spin Contributions to the Zero-Field Splitting Tensor in Organic Triplets, Carbenes, and Biradicals. A Density Functional and ab Initio Study. *J. Phys. Chem. A* **2006**, *110*, 12267−12275.

(21) Ganyushin, D.; Neese, F. First-Principles Calculations of Zero-Field Splitting Parameters. *J. Chem. Phys.* **2006**, *125*, 024103 1−10.

(22) Ganyushin, D.; Gilka, N.; Taylor, P. R.; Marian, C. M.; Neese, F. The Resolution of the Identity Approximation for Calculations of Spin−Spin Contribution to Zero-Field Splitting Parameters. *J. Chem. Phys.* **2010**, *132*, 144111 1−11.

(23) Misochko, E. Ya.; Korchagin, D. V.; Bozhenko, K. V.; Chapyshev, S. V.; Aldoshin, S. M. A Density Functional Theory Study of the Zero-Field Splitting in High-Spin Nitrenes. *J. Chem. Phys.* **2010**, *133*, 064101 1−10.

(24) Glendening, E. D.; Badenhoop, J. K.; Reed, A. E.; Carpenter, J. E.; Bohmann, J. A.; Morales, C. M.; Landis, C. R.; Weinhold, F. *NBO 6.0*; Theoretical Chemistry Institute, University of Wisconsin: Madison, WI, 2013.

(25) Mayer, I. Bond Orders and Valences from ab Initio Wave Functions. *Int. J. Quantum Chem.* **1986**, *29*, 477−483.

(26) Nakano, Y.; Yagyu, T.; Hirayama, T.; Ito, A.; Tanaka, K. Synthesis and Intramolecular Magnetic Interaction of Triphenylamine Derivatives with Nitronyl Nitroxide Radicals. *Polyhedron* **2005**, *24*, 2141−2147.

(27) Stoll, S.; Schweiger, A. J. EasySpin, a Comprehensive Software Package for Spectral Simulation and Analysis in EPR. *J. Magn. Reson.* **2006**, *178*, 42−55.

(28) Borden, W. T.; Davidson, E. R. Singlet−Triplet Energy Separations in Some Hydrocarbon Diradicals. *Annu. Rev. Phys. Chem.* **1979**, *30*, 125−153.

(29) Sherrill, C. D. In *Annual Reports in Computational Chemistry*; Spellmeyer, D., Ed.; Elsevier: Amsterdam, The Netherlands, 2005; Vol. *1*, pp 45−54.

(30) Szalay, P. G.; Muller, T.; Gidafalvi, G.; Lischka, H.; Shepard, R. Multiconfigurational Self-Consistent Field and Multireference Configuration Interaction Methods and Applications. *Chem. Rev.* **2012**, *112*, 108−181.

(31) Slipchenko, L.; Krylov, A. Electronic Structure of the Trimethylenemethane Diradical in its Ground and Electronically Excited States: Bonding, Equilibrium Geometries, and Vibrational Frequencies. *J. Chem. Phys.* **2003**, *118*, 6874−6883.

(32) Mozhayskiy, V.; Goebbert, D.; Velarde, L.; Sanov, A.; Krylov, A. Electronic Structure and Spectroscopy of Oxyallyl: A Theoretical Study. *J. Phys. Chem. A* **2010**, *114*, 6935−6943.

(33) Unfortunately, the NBO-6 program package does not provide the NRT analysis for certain types of open-shell wave functions (e.g., CAS wave functions).

(34) Noodleman, L. Valence Bond Description of Anti-Ferromagnetic Coupling in Transition-Metal Dimers. *J. Chem. Phys.* **1981**, *74*, 5737−5743.
(35) Noodleman, L.; Davidson, E. R. Ligand Spin Polarization and Antiferromagnetic Coupling in Transition Metal Dimmers. *Chem. Phys.* **1986**, *109*, 131−143.
(36) Yamaguchi, K.; Takahara, Y.; Fueno, T. In *Applied Quantum Chemistry*; Smith, V. H., Ed.; Reidel: Dordrecht, The Netherlands, 1986, pp 82−215.